Ursodeoxycholic acid and its taurine/glycine conjugated species reduce colitogenic dysbiosis and equally suppress experimental colitis in mice

Lien Van den Bossche[1], Pieter Hindryckx[1], Lindsey Devisscher[1], Sarah Devriese[1], Sophie Van Welden[1], Tom Holvoet[1], Ramiro Vilchez-Vargas[2], Marius Vital[3], Dietmar H. Pieper[3], Julie Vanden Bussche[4], Lynn Vanhaecke[4], Tom Van de Wiele[2], Martine De Vos[1] and Debby Laukens[1#]

[1]Department of Gastroenterology, Ghent University, Ghent, Belgium; [2]Center for Microbial Ecology and Technology, Ghent University, Ghent, Belgium; [3]Microbial Interactions and Processes Research Group, Department of Medical Microbiology, Helmholtz Centre for Infection Research (HZI), Braunschweig, Germany; [4]Laboratory of Chemical Analysis, Department of Veterinary Public Health and Food Safety, Faculty of Veterinary Medicine, Ghent University, Ghent, Belgium

Running title: UDCA and its conjugates reduce colitogenic dysbiosis

#Address correspondence to: Debby Laukens, debby.laukens@ugent.be.

ABSTRACT

The promising results with secondary bile acids in experimental colitis suggest that they may represent an attractive and safe class of drugs for the treatment of inflammatory bowel diseases (IBD). However, the exact mechanism by which bile acid therapy confers protection from colitogenesis is currently unknown. Since the gut microbiota plays a crucial role in the pathogenesis of IBD, and exogenous bile acid administration may affect the community structure of the microbiota, we examined the impact of the secondary bile acid ursodeoxycholic acid (UDCA) and its taurine/glycine conjugates on the fecal microbial community structure during experimental colitis. Daily oral administration of UDCA, tauroursodeoxycholic acid (TUDCA) or glycoursodeoxycholic acid (GUDCA) equally lowered the severity of dextran sodium sulfate-induced colitis in mice, as evidenced by reduced body weight loss, colonic shortening and expression of inflammatory cytokines. Illumina sequencing demonstrated that bile acid therapy during colitis did not restore fecal bacterial richness and diversity. However, bile acid therapy normalized the colitis-associated increased ratio of *Firmicutes* to *Bacteroidetes*. Interestingly, administration of bile acids prevented the loss of *Clostridium* cluster XIVa and increased the abundance of *Akkermansia muciniphila,* bacterial species known to be particularly decreased in IBD patients. We conclude that UDCA, which is an FDA-approved drug for cholestatic liver disorders, could be an attractive treatment option to reduce dysbiosis and improve inflammation in human IBD.

IMPORTANCE

Secondary bile acids are emerging as attractive candidates for the treatment of inflammatory bowel disease. Although bile acids may affect the intestinal microbial community structure, which significantly contributes to the course of these inflammatory disorders, the impact of bile

47 acid therapy on the fecal microbiota during colitis has not yet been considered. Here, we studied
48 the alterations in the fecal microbial abundance in colitic mice following the administration of
49 secondary bile acids. Our results show that secondary bile acids reduce the severity of colitis and
50 improve colitis-associated fecal dysbiosis at the phylum level. This study indicates that secondary
51 bile acids might act as a safe and effective drug for inflammatory bowel disease.
52
53 **INTRODUCTION**
54 Inflammatory bowel diseases (IBD) are chronic inflammatory disorders of the gastrointestinal
55 tract characterized by intestinal dysbiosis. Restricted bacterial diversity and underrepresentation
56 of anti-inflammatory microorganisms such as *Clostridium* cluster XIVa and *Akkermansia*
57 *muciniphila* represent typical dysbiotic features in IBD (1–4). Since the intestinal microbial
58 community performs a wide range of bile acid modifications including deconjugation,
59 dehydroxylation, oxidation and epimerization (5), shifts in the composition of the gut microbiota
60 are associated with perturbations of the fecal bile acid profile (6, 7). Of particular interest, Duboc
61 and colleagues demonstrated that the conversion of primary bile acids (synthesized in the liver
62 from cholesterol) to secondary bile acids (generated by bacterial modifications) is impaired in
63 IBD patients (7). Because secondary bile acids exhibit immunomodulatory functions (7–10),
64 increasing secondary bile acid levels in the intestinal lumen could be an efficient therapeutic
65 approach for IBD. In line with this hypothesis, the administration of the secondary hydrophilic
66 bile acid ursodeoxycholic acid (UDCA) ameliorates experimental colitis but the exact mechanism
67 protecting from colitogenesis is not fully understood (11).
68 When administered orally, unconjugated UDCA is rapidly conjugated with glycine in humans,
69 and to a lesser extent with taurine, on its first pass through the liver (12, 13). Based on the
70 observation that fecal bile acid hydrophobicity correlates with the severity of colitis (14), it is

reasonable to assume that conjugates of UDCA, which are more hydrophilic than unconjugated UDCA, might be more favorable therapeutic agents for intestinal inflammation. In this regard, we and others have shown that tauroursodeoxycholic acid (TUDCA) alleviates dextran sodium sulfate (DSS)-induced colitis in mice (15, 16). The potential beneficial effect of glycoursodeoxycholic acid (GUDCA) in colitis, however, has not been addressed so far and studies comparing the therapeutic effectiveness of these different bile acid species are lacking.

While the composition of the luminal bile acid pool is controlled by intestinal bacteria, it is well established that bile acids, in turn, also shape the gut microbiota. Bile acids restrict bacterial proliferation and overgrowth directly by causing membrane damage, which is positively correlated with bile acid hydrophobicity (17–19). Thus, the bactericidal activity of bile acids decreases with increasing numbers of hydroxyl groups and by conjugation of the bile acid side chain with taurine or glycine (19). In addition to their role as antimicrobial agents, bile acids also stimulate the growth of selected bacterial species (5). Similarly, these properties are determined both by the hydroxylation pattern and the conjugation status of the bile acid steroid nucleus. For example, increased intestinal levels of bile acids carrying a hydroxyl group at position C7 of the steroid core favor the growth of 7α-dehydroxylating bacteria, such as *Clostridium* cluster XIVa members (20, 21). Furthermore, the amino acids in conjugated bile acids act as microbial substrates for distinct bacterial groups; glycine is metabolized by *Clostridium* species (22, 23), while taurine is a source of sulphite from which *Bilophila wadsworthia* derives energy for its growth (24, 25). Interestingly, a diet high in saturated fat promotes taurine-conjugation of hepatic bile acids, resulting in the outgrowth of *B. wadsworthia* and exacerbation of colitis (26).

Considering that the gut microbial architecture and metabolism contribute to the course of IBD (27, 28), we compared the therapeutic effectiveness of UDCA and its taurine/glycine conjugates in DSS-induced colitis in mice and investigated their impact on the fecal microbial community.

95

96 **MATERIALS AND METHODS**

97 **Animals.** Male 8-week-old C57Bl/6J mice were obtained from Harlan (Harlan Laboratories,
98 Horst, The Netherlands) and maintained under standard laboratory conditions with *ad libitum*
99 access to food (mice maintenance chow, Carfil Labofood, Pavan Service, Belgium) and water.
100 Prior to the experiment, mice were co-housed to homogenize gut microbiota between
101 experimental groups. After a one-week acclimatization, mice were assigned to the treatment
102 groups based on body weights. In order to avoid bacterial cross-contamination between groups,
103 mice of different treatment groups were housed in separate cages. The study was approved by the
104 Institutional Review Board of the Faculty of Medicine and Health Science of Ghent University
105 (ECD 2014-25).

106 **Bile acid treatment.** Mice were divided into five groups (n = 8 in each group). Three of them
107 received bile acid treatment: UDCA (Tokyo Chemical Industry Co. Ltd, Toshima-Ku, Tokyo,
108 Japan), TUDCA (Calbiochem, Darmstadt, Germany) or GUDCA (Sigma-Aldrich, Diegem,
109 Belgium). Bile acids were dissolved in phosphate-buffered saline (PBS) or Labrafil® M1944
110 (Gattefosse, Saint-Priest Cedex, France) and administered daily by oral gavage (500 mg/kg/day).
111 Treatments started at day 0 of DSS exposure. A non-DSS control group and DSS control group
112 (referred to as placebo-treated group) received the vehicle (PBS or Labrafil®) alone.

113 **Induction and assessment of colitis.** Acute colitis was established by adding 4% (w/v) DSS
114 (molecular weight 36,000–50,000; MP Biomedicals, Illkirch, France) to the drinking water for 7
115 days, followed by normal water for 3 days. A non-DSS control group received normal drinking
116 water throughout the experiment. Body weight and disease activity were recorded daily. A
117 disease activity index (DAI) was calculated as the combined score of body weight loss (0, none;
118 1, 0-10%; 2, 10-20%; 3, >20%), stool consistency (0, normal droppings; 1, loose droppings; 2,

119 diarrhea) and fecal blood loss (0, none; 1, hemoccult positive; 2, gross bleeding). Occult blood
120 was detected using the Coloscreen Hemoccult kit (Helena Laboratories Inc., Beaumont, Texas,
121 USA). Ten days after initiation of the experiment, mice were anesthetized and blood was
122 collected from the retro-orbital sinus. The mice were then sacrificed by cervical dislocation, the
123 colons were removed and their lengths were measured. Segments of distal colon were cut, rinsed
124 with PBS and frozen in liquid nitrogen. The blood was centrifuged (10.000 rpm for 10 min at
125 4°C) and serum was collected. All samples were stored at -80°C until further processing.
126 **Luminex.** Colonic tissues were homogenized in PBS containing protease and phosphatase
127 inhibitors and total protein concentration was measured using the Bradford method (Bio-Rad,
128 Nazareth, Belgium). Protein levels of chemokine (C-X-C motif) ligand 1 (CXCL1), granulocyte
129 colony-stimulating factor (G-CSF) and interleukin (IL)-6 were determined in colon homogenates
130 and serum using the Bio-Plex Pro Mouse Cytokine Group I multiplex kit (Bio-Rad), according to
131 the manufacturer's instructions. Measurements were performed with the Bio-Plex MAGPIX
132 Multiplex Reader and data were analyzed using the Bio-Plex Manager 6.1 software (Bio-Rad).
133 **DNA extraction from fecal samples.** Fresh fecal pellets were collected at day 9 of colitis and
134 immediately stored at -80°C. Total DNA was extracted from the fecal samples using the QIAamp
135 DNA Stool Mini Kit (Qiagen Benelux, Venlo, The Netherlands). First, 180 to 220 mg of stool
136 was resuspended in 1.4 ml buffer ASL. Then, 0.5 g 0.1 mm Zirconia beads (Biospec Products,
137 Bartlesville, Oklahoma) and 4 glass beads (Biospec Products) were added and samples were
138 homogenized by vortexing. The suspension was then heated at 95°C for 15 min and the
139 manufacturer's instructions were followed.
140 **Illumina sequencing.** The V1-2 region of the 16S rRNA gene was amplified as previously
141 described (29). Briefly, in a first 20 cycle polymerase chain reaction (PCR) reaction, the 16S
142 rRNA gene target was enriched using the well-documented 27F and 338R primers (30, 31) as

143 previously specified (32). This reaction mixture was used as template in a second 15 cycle PCR
144 reaction with primers comprising sequences complementary to the Illumina specific adaptors to
145 the 5'-ends (29). The latter reaction mixture was then used as template in a third 10 cycle PCR
146 reaction with primers designed to integrate both the sequence of the specific Illumina
147 multiplexing sequencing primers and the index primers. Libraries prepared by pooling equimolar
148 ratios of amplicons were finally sequenced on a MiSeq (Illumina, Hayward, CA, USA).
149 Afterwards, reads were annotated as described by Verstraelen et al. (33).
150 **Illumina data analysis.** Data-analysis was performed as previously described (33). After
151 resampling to the minimum sequencing depth using the phyloseq package (34) from the R
152 program (35), a total of 8,911 reads were obtained. Rarefaction curves were generated using the
153 vegan package from R (36). All phylotypes were assigned a taxonomic affiliation based on the
154 naive Bayesian classification (RDP classifier) (37) with a threshold of 80%. Relative abundances
155 of all phylotypes were then compared between different experimental groups.
156 **Quantitative real-time PCR (qRT-PCR).** Total fecal DNA was diluted 1:2 in water and 3 µl
157 was used in qRT-PCR with SYBR Green (SensiMix™ SYBR No-ROX Kit, Bioline Reagents,
158 UK) and 250 nM of each primer (BioLegio, Nijmegen, The Netherlands). Primer sequences used
159 for amplification of *A. muciniphila* were 5'-CAGCACGTGAAGGTGGGGAC-3' and 5'-
160 CCTTGCGGTTGGCTTCAGAT-3' (38). A two-step program was performed on the LightCycler
161 480 (Roche). Cycling conditions were 95°C for 10 min, 45 cycles of 95°C for 10 s and 60°C for 1
162 min. The amount of *A. muciniphila* 16S rRNA gene in each sample was normalized to the total
163 amount of bacterial 16S rRNA gene. For the quantification of total 16S rRNA gene copies, fecal
164 DNA was diluted 1:10 in water and the universal bacterial 16S rRNA gene primers PRBA338f
165 5'-ACTCCTACGGGAGGCAGCAG-3' and PRUN518r 5'-ATTACCGCGGCTGCTGG-3' were

166 used (39). Total bacterial load was calculated using the formula $2^{deltaCt}$ / [total DNA
167 concentration].

168 **Bile acid quantification.**

169 ***Sample preparation.*** Fresh fecal pellets were collected at day 4 of colitis and immediately stored
170 at -80°C. Before bile acids were extracted from fecal samples, 20 µl of an internal standard
171 solution (TUDCA-d5 (Santa-Cruz Biotechnology, Heidelberg, Germany) at 25 ng/µl in methanol
172 (VWR International, Merck Millipore, Darmstadt, Germany)) was added to 25 mg feces. The
173 extraction protocol started with the addition of 5 ml ice-cold acetonitrile (VWR International)
174 containing 5% ammonium hydroxide (Merck Millipore, Darmstadt, Germany). The solution was
175 homogenized with an Ultra-Turrax homogenizer, thoroughly mixed by vortexing for 1 min and
176 then placed in an ultrasonic bath for 30 min. The resultant mixture was centrifuged at 9,000 x g
177 for 10 min and supernatant was collected. The extraction procedure was repeated once more and
178 the combined supernatants were subsequently evaporated under nitrogen at 40°C. Each dry
179 extract was then resuspended in 200 µl of a 40:60 mixture of solvent A (7.5 mM ammonium
180 acetate (Merck Millipore) in ultrapure water, pH 4.0) and solvent B (5% acetonitrile in
181 methanol), centrifuged at 9,000 x g for 10 min and supernatant was collected. To compensate for
182 matrix effects, the standard addition method was applied for bile acid quantification (40). Briefly,
183 supernatant was divided into two equal aliquots and transferred to liquid chromatography-mass
184 spectrometry vials. One aliquot was spiked with 20 µl of the 40:60 mixture of solvent A and B.
185 The other aliquot was spiked with 20 µl of bile acid solution (a 40:60 mixture of solvent A and B,
186 supplemented with 16.5 ng/µl lithocholic acid (LCA; Sigma-Aldrich), 89.4 ng/µl UDCA (Simga-
187 Aldrich), 0.75 ng/µl TUDCA (Calbiochem) and 0.75 ng/µl GUDCA (Sigma-Aldrich)). A 10 µl
188 aliquot of each sample was injected into the ultra-high performance liquid chromatography with
189 high resolution mass spectrometry (UHPLC-HRMS) system.

190 ***UHPLC-HRMS analysis.*** Chromatographic separation of bile acids was carried out on an Accela
191 UHPLC system of Thermo Fisher Scientific (San José, CA, USA), with an Acquity UPLC HSS
192 C18 column (1.8 µm, 50 mm × 2.1 mm, Waters). The binary solvent system consisting of two
193 solvents A and B was set at a constant flow rate of 300 µl/min at 35°C. For elution, a gradient
194 profile was applied with the following proportions (v/v) of solvent A: 0 – 1.0 min at 40%, 1.0 –
195 6.0 min from 40% to 1%, 6.0 – 8.0 min at 1%, 8.0 – 8.1 min from 1% to 40%, followed by 3.9
196 min of re-equilibration.
197 HRMS analysis was performed on an Exactive^{TM} stand-alone benchtop mass spectrometer
198 (Thermo Fisher Scientific), equipped with a heated electrospray ionization source (HESI-II),
199 operating in the negative ionization mode. Ionization source working parameters were optimized
200 and were set to a sheath, auxiliary and sweep gas of 40, 5 and 1 arbitrary units (au), respectively,
201 heater and capillary temperature of 120°C and 375°C and tube lens, skimmer, capillary and spray
202 voltage of 123 V, 22 V, 43.5 V and 4 kV (+/-), respectively. A scan range of *m/z* 300-550 was
203 selected and the resolution was set at 100,000 FWHM at 1 Hz (1 scan per second). The automatic
204 gain control (AGC) target was set at high dynamic range (3 × E^6 ions) and the maximum
205 injection time was 100 ms.
206 ***Data processing.*** HRMS data processing was performed with Xcalibur™ 3.0 (Thermo Fisher
207 Scientific). The concentration of a selected bile acid was calculated using the following formula
208 (40):

$$C_{unk} = \frac{C_{SA} \times AR_{unk}}{AR_{SA} - AR_{unk}}$$

209 with C_{unk} being the unknown concentration of the bile acid in the original fecal sample, C_{SA} being
210 the spiked concentration of the bile acid in the fecal sample after standard addition, AR_{unk} being

211 the area ratio of the bile acid in the original sample and AR_{SA} being the area ratio of the bile acid
212 in the fecal sample after standard addition.

213 **Statistical analysis.** Statistical analysis was performed using SPSS Statistics version 22.0 (IBM
214 SPSS, Chicago, USA) and GraphPad Prism version 4 (GraphPad, California, USA). All data are
215 expressed as mean ± SEM. Data were tested for normality using the Kolmogorov-Smirnov test.
216 Statistical significant differences between groups were assessed using the unpaired Student's t-
217 test for normally distributed data, applying the Welch's correction in case of unequal variances,
218 or the Mann-Whitney U test for non-normally distributed data. Two-tailed probabilities were
219 calculated and P-values of less than 0.05 were considered statistically significant.

220 **Nucleotide sequence accession number.** The sequence data were submitted to the European
221 Nucleotide Archive (ENA) with accession numbers from LT700235 to LT702885 and can be
222 accessed at http://www.ebi.ac.uk/ena/data/view/LT700235-LT702885.

223

224 **RESULTS**

225 **Oral administration of UDCA or its taurine/glycine conjugated species is equally protective**
226 **in acute DSS-induced colitis**

227 To compare the therapeutic effects of UDCA and its taurine/glycine derivatives on DSS-induced
228 colitis, C57BL6/J mice were challenged with 4% DSS for 7 days and treated daily with UDCA,
229 TUDCA or GUDCA by oral gavage. Bile acid therapy reduced the rate of body weight loss, with
230 no differences in efficacy between the three bile acid treatments (Figure 1A). At day 10 after the
231 initiation of colitis, body weight loss was significantly higher in placebo-treated mice than in bile
232 acid-treated mice (P=0.027; P=0.021 and P=0.021 for treatment with UDCA, TUDCA and
233 GUDCA, respectively). Accordingly, the clinical disease activity score, colonic shortening and
234 colonic concentrations of CXCL1, G-CSF and IL-6, which have been reported to show enhanced

235 expression in the acute phase of DSS-induced colitis (41, 42), were all attenuated following bile
236 acid treatment (Figure 1B-D). At the systemic level, lower levels of CXCL1 and G-CSF, but not
237 IL-6, were detected in the serum of bile acid-treated mice as compared with the placebo-treated
238 group (Figure 1E). Together, these data demonstrate that UDCA and its taurine/glycine
239 conjugates decrease the severity of DSS-induced colitis with similar effectiveness.
240
241 **Bile acid supplementation to mice challenged with DSS prevents colitis-associated dysbiosis**
242 **at the phylum level**
243 Because bile acids have been recognized as modulators of the intestinal microbiota (21, 26),
244 which is believed to play a critical role in colitis (1, 28), we questioned whether administration of
245 UDCA or its conjugated derivatives prevented dysbiosis during experimental colitis. Fecal
246 samples were collected two days after removing DSS from the drinking water (day 9), when
247 colitis was fully established, and microbiota profiles were determined by 16S rRNA Illumina
248 MiSeq sequencing. Four out of 40 mice were excluded from microbiota analysis because of
249 insufficient amounts of feces available for DNA extraction. As expected, administration of DSS
250 resulted in a significant reduction of species richness (number of operational taxonomic units;
251 P=0.002; Figure 2A) and microbial diversity (Shannon index; takes into account both species
252 abundance and evenness; P=0.002; Figure 2B). In addition, the total fecal bacterial load had
253 dropped significantly to 22% of values seen in non-DSS control mice (P=0.002; Figure 2C).
254 Compared to the placebo-treated group, microbial richness and diversity were slightly declined
255 when colitic mice were treated with UDCA (P=0.086 and P=0.015, respectively), but no changes
256 could be observed after the administration of TUDCA or GUDCA. Furthermore, daily
257 administration of UDCA or its taurine/glycine conjugates during colitis did not affect the
258 decrease in fecal bacterial load (Figure 2A-C).

We next analyzed the fecal microbial composition at the major taxonomic hierarchy levels to determine if particular bacterial phyla were altered following bile acid therapy during active disease. Taxonomic assignment of the sequence reads revealed two dominant phyla, *Bacteroidetes* and *Firmicutes*, accounting for respectively 58.31% and 31.05% in fecal communities of non-DSS control mice. Other phyla present with an average relative abundance ranging from 4.50% to 0.09% were *Proteobacteria, Deferribacteria, Candidatus Saccharibacteria* and *Actinobacteria*. Administration of DSS significantly altered the structure of the fecal microbiome. At day 9 of colitis, the *Firmicutes/Bacteroidetes* ratio increased in mice that were challenged with DSS (Figure 2D). More specifically, bacteria of the *Bacteroidetes* phylum were underrepresented in fecal samples of placebo-treated mice while the relative abundance of *Firmicutes* bacteria tended to increase (Figure 2E). Interestingly, oral administration of TUDCA or UDCA normalized the *Firmicutes/Bacteroidetes* ratio, while GUDCA treatment showed a slight but non-significant tendency to reduce this ratio (P=0.12, Figure 2D). Compared to placebo-treated mice, the fecal microbial community of bile acid-treated mice with colitis showed a lower abundance of *Firmicutes* and an increased abundance of *Bacteroidetes* (Figure 2E). These results show that bile acid therapy in DSS-induced colitis neither mitigate nor aggravate altered microbial richness and population diversity but corrects fecal microbiota dysbiosis at the phylum level.

Bile acid supplementation to mice challenged with DSS alters the fecal microbiota at lower taxonomic levels

To examine which bacterial populations accounted for the changes at phylum level, we investigated the relative abundance of bacteria at lower taxonomic levels. The abundance of unclassified *Bacteroidetes* was reduced upon DSS administration, whereas no changes were

noted for *Bacteroidia* levels (Figure 3A). Interestingly, bile acid supplementation did not elicit an effect on unclassified *Bacteroidetes* but was associated with a significant increase in the abundance of *Bacteroidia* compared with placebo-treated mice (Figure 3A). Examination at the family level indicated that upon DSS challenge, the relative proportion of *Bacteroidaceae* and *Porphyromonadaceae* increased (Figure 3B and C), while *Prevotellaceae* family members nearly completely disappeared in fecal samples of placebo-treated mice (0.03% vs. 6.64% in non-DSS control mice, Figure 3D). Interestingly, the relative abundance of *Prevotellaceae* increased to 2.24% and 2.61% when mice were treated with UDCA or TUDCA, respectively (Figure 3D). Moreover, *Bacteroidaceae* tended to further increase upon bile acid supplementation, especially when mice were treated with UDCA (Figure 3B). Within *Firmicutes*, *Erysipelotrichia* expanded in the fecal samples of mice that were challenged with DSS, though bile acid therapy did not abrogate nor amplify this increase (Figure 3A). However, the relative abundance of *Clostridia* remained unchanged in the placebo-treated group, but declined in mice that were administered UDCA or derivatives (Figure 3A). Comparisons at the genus level further demonstrated that DSS-induced colitis was associated with the outgrowth of *Clostridium* clusters XI and XIVb and with a depletion of *Clostridium* cluster XIVa (Figure 3E; data not shown). As compared to the placebo-treated group, colitic mice that were treated with UDCA or conjugates exhibited increased numbers of *Clostridium* cluster XIVa bacteria (Figure 3E). *Clostridium* species belonging to the clusters XI and XIVb, however, were not altered upon bile acid treatment (data not shown). Interestingly, sequences that were aligned to the *Verrucomicrobia* phylum were completely absent in the fecal communities of non-DSS control mice. Within this phylum, however, one genus *(Akkermansia)* expanded in the fecal samples of mice that were challenged with DSS. *Akkermansia* accounted for 0.047% of the detectable bacteria in the fecal samples of placebo-treated mice and the relative abundance further increased upon treatment with UDCA,

307 TUDCA or GUDCA (0.145%, 0.114% and 0.159%, respectively; Figure 3F). Given the
308 importance of these species in IBD (3, 4), the bile acid-induced enrichment of *A. muciniphila* was
309 confirmed by qRT-PCR analysis (Figure 3G).
310
311 **Oral administration of UDCA, TUDCA and GUDCA results in a similar fecal bile acid pool**
312 To compare the extent of biotransformation of orally administered UDCA, TUDCA and
313 GUDCA, we performed UHPLC-HRMS analysis on fecal samples collected at day 4 of colitis.
314 This time point was chosen because changes in the bile acid composition have been suggested to
315 reach a steady-state already within 4 days of bile acid administration (43). Due to insufficient
316 quantities of feces, two mice were excluded from UHPLC-HRMS analysis. UDCA
317 concentrations were significantly higher in fecal samples of mice administered UDCA or its
318 taurine/glycine conjugates than in those of placebo-treated mice (Figure 4A). Concomitant with
319 these changes, we observed increased fecal levels of TUDCA and LCA in bile acid-treated mice
320 (Figure 4B and C). Of note, these changes occurred irrespective of whether animals were treated
321 with UDCA, TUDCA or GUDCA and without significant differences between the three bile acid
322 treatments. In contrast, administration of GUDCA caused a substantial increase in fecal GUDCA
323 levels, while no elevation was observed in animals that were administered UDCA or TUDCA
324 (Figure 4D). This finding is consistent with the fact that bile acids are predominantly conjugated
325 with taurine (>97%), instead of glycine (<0.1%), in mice (44). Together, these data indicate that
326 orally administered UDCA, TUDCA and GUDCA are extensively metabolized *in vivo*, resulting
327 in a similar fecal bile acid composition.
328
329 **DISCUSSION**

330 Previous studies have reported the therapeutic potential of the hydrophilic bile acids UDCA and
331 TUDCA in experimental colitis (11, 15, 16), albeit without comparing their respective
332 effectiveness. In the present study, we showed that daily administration of UDCA and its taurine-
333 and glycine-coupled conjugates equally attenuated body weight loss, disease activity and colonic
334 shortening caused by DSS. Moreover, oral bile acid therapy reduced pro-inflammatory cytokine
335 concentrations in the colon and serum to a similar extent.
336 Bile acids are important regulators of the intestinal microbiota (21), which plays a crucial role in
337 the pathogenesis of IBD (27). In order to examine the role of UDCA and its taurine/glycine
338 conjugated species in the regulation of the intestinal microbiota during colitis, we orally
339 administered UDCA, TUDCA or GUDCA to mice that were challenged with DSS and
340 determined fecal microbiota profiles by 16S rRNA Illumina MiSeq sequencing. Consistent with
341 previous studies, DSS-induced colitis was associated with distinct alterations in the population
342 structure of the gut microbiota (45, 46). These changes were generally characterized by a reduced
343 overall microbial diversity and a decrease in species richness and bacterial load, which are also
344 main hallmarks of dysbiosis in IBD patients (47, 48). We showed that oral bile acid
345 administration did not prevent the DSS-induced changes in microbial richness, diversity, and
346 bacterial load. Interestingly, species diversity decreased even more when colitic mice were
347 treated with UDCA. However, although reduced richness and diversity of the gut microbiota have
348 been associated with human disease (49–51), it seems unlikely that this effect is also clinically
349 relevant; the clinical outcome in UDCA-treated mice was similar to that of mice that were treated
350 with TUDCA or GUDCA.
351 At the phylum level, TUDCA, UDCA, and to a lesser extent GUDCA, normalized the
352 *Firmicutes/Bacteroidetes* ratio that was increased in placebo-treated mice with colitis. This ratio
353 is often used as a proxy for microbial health status (52–57) and, more specifically, to describe the

354 degree of dysbiosis in IBD (55–57). Of note, the phylum-level population shifts from
355 *Bacteroidetes* to *Firmicutes* induced by DSS in our study resemble those observed in obese
356 individuals and in animals on a high-fat diet, and have been associated with low-grade intestinal
357 and systemic inflammation in obesity (58, 59). In this context, fecal calprotectin and plasma C-
358 reactive protein levels showed a positive correlation with bacteria belonging to the *Firmicutes*,
359 whereas a negative correlation was found between C-reactive protein levels and specific groups
360 within the *Bacteroidetes* (58). It is therefore likely that bile acid therapy counteracts the
361 development of a "pro-inflammatory" microbiota during colitis. This is speculative since it
362 remains unknown if the changes seen in the *Firmicutes/Bacteroidetes* ratio following bile acid
363 treatment are a cause, rather than a consequence, of the bile acid anti-inflammatory effect.
364 However, bile acid therapy did not prevent the DSS-induced decrease in unclassified members of
365 the phylum *Bacteroidetes* but increased the relative abundance of *Bacteroidia*, which was not
366 affected by DSS. Thus, we can speculate that bile acid therapy directly interferes with an
367 imbalanced microbial environment.
368 We demonstrated that *Clostridium* cluster XIVa species were significantly underrepresented upon
369 DSS challenge, confirming previous observations in both human and experimental IBD (2, 60–
370 62). However, oral administration of UDCA or its taurine/glycine conjugates was able to provoke
371 an enrichment of these species compared with placebo-treated mice. It has been shown that
372 selected members within the clostridial cluster XIVa possess 7α-dehydroxylation activity (20),
373 which is involved in a multistep biochemical pathway converting UDCA to LCA (63, 64). In our
374 experiment, orally administered TUDCA and GUDCA were rapidly deconjugated to UDCA, so
375 either bile acid treatment created a substrate-rich environment for these species. This may explain
376 the bloom of *Clostridium* cluster XIVa that was observed in colitic mice that were treated with
377 bile acids. *Clostridium* spp. belonging to cluster XIVa are important inducers of regulatory T

cells in the colon (65). In addition, 80% of the butyrate-producing strains isolated from human fecal samples belong to the clostridial cluster XIVa (66). Butyrate is a short-chain fatty acid with distinctive anti-inflammatory properties that has already proven its efficacy in Crohn's disease (67). However, butyrate-producing bacteria are depleted in the fecal microbiota of IBD patients (61, 62, 68). Thus, our observation that UDCA or its taurine/glycine conjugates increased the abundance of *Clostridium* cluster XIVa during colonic inflammation is of particular interest and may suggest an immunomodulatory role of these bile acids.

Another finding of this study was the overrepresentation of *Bacteroidaceae*, *Prevotellaceae* and *Akkermansia* in fecal samples of bile acid-treated mice following DSS exposure. These results might be related to the stimulatory effect of bile acids on mucin secretion as a defense mechanism to protect the gastrointestinal epithelium against potential bile acid toxicity (69–71). Bacterial species belonging to the genera *Bacteroides*, *Prevotella* and *Akkermansia* produce one or more enzymes required for mucin degradation (72), which is enhanced during the acute phase of DSS-induced colitis (46). Therefore, it is reasonable to assume that these bacteria can grow better in an environment that is, resulting from exogenous bile acid administration, enriched with mucins. *A. muciniphila* is a commensal bacterium residing in the mucus layer of the intestinal tract and has been shown to be reduced in IBD patients (3, 4). Although conflicting results were obtained in studies assessing the role of *Akkermansia* in colonic inflammation, these species are thought to play a key role in the regulation of gut barrier function and mucosal immune responses toward the commensal microbiota (73, 74).

The molecular structure of a bile acid determines its metabolism, physicochemical properties and biological effects (75). In the present study, we used three bile acids sharing the same steroidal hydroxylation pattern but differing in their amino acid conjugation pattern. Neither bile acid species tested proved to be more or less efficacious than the other in reducing colonic

inflammation. Likewise, administration of UDCA induced similar changes in the bacterial community compared with its taurine/glycine conjugated species. These observations can be explained by the rapid *in vivo* biotransformation of orally administered bile acids by the liver and by the intestinal microbiota. With the exception of fecal GUDCA concentrations, which were only increased following GUDCA therapy, there were no differences in fecal concentrations of UDCA, TUDCA or LCA between mice that were administered UDCA or its conjugates. This is in contrast with data from previous studies in patients with primary biliary cirrhosis (12) and rats (43) showing that, compared with UDCA, orally administered TUDCA undergoes reduced 7-dehydroxylation to LCA. It is conceivable that interspecies differences in intestinal microbiota account for these discrepancies. For example, deconjugation of TUDCA or GUDCA is a prerequisite for further 7-dehydroxylation and is catalyzed by bile salt hydrolases (43). Because *Lactobacilli,* which express bile salt hydrolases, are more abundant in the mouse gut microbiota as compared to the human gut microbiota (76), it is likely that biotransformation of these conjugated bile acids occurs to a larger extent in mice.

In summary, we report that UDCA and its taurine/glycine conjugated species ameliorate colonic inflammation in mice without differing in therapeutic effectiveness, and reduce DSS-induced fecal dysbiosis at the phylum level, irrespective of the bile acid conjugation status. As we demonstrated no advantage of using either the taurine or glycine conjugate of UDCA, we suggest that UDCA could be a safe and readily available treatment option for IBD. This conclusion is further supported by the current therapeutic use of UDCA in cholestatic patients (77) and by its preventive effects on IBD-associated colorectal carcinogenesis (78–80).

ACKNOWLEDGEMENTS

The authors are grateful to Dr. Falk Pharmaceuticals, who kindly provided TUDCA for research purposes. We would also like to thank Hilde Devlies, Griet Driesschaert and Petra Van Wassenhove for providing technical assistance. There are no conflicts of interest to declare.

FUNDING INFORMATION

This work was supported by research grants from the Research Foundation Flanders (FWO; 11J9915N and 1298213N), a concerted action grant (GOA) from the Special Research Fund (BOF; GOA 2012/01G00812) of Ghent University, and a grant from the Belgian foundation for Crohn's disease and ulcerative colitis patients (CCV vzw, research grant 2014).

REFERENCES

1. **Nagao-Kitamoto H**, **Kitamoto S**, **Kuffa P**, **Kamada N**. 2016. Pathogenic role of the gut microbiota in gastrointestinal diseases. Intest Res **14**:127–138.

2. **Andoh A**, **Imaeda H**, **Aomatsu T**, **Inatomi O**, **Bamba S**, **Sasaki M**, **Saito Y**, **Tsujikawa T**, **Fujiyama Y**. 2011. Comparison of the fecal microbiota profiles between ulcerative colitis and Crohn's disease using terminal restriction fragment length polymorphism analysis. J Gastroenterol **46**:479–486.

3. **Png CW**, **Lindén SK**, **Gilshenan KS**, **Zoetendal EG**, **McSweeney CS**, **Sly LI**, **McGuckin MA**, **Florin THJ**. 2010. Mucolytic bacteria with increased prevalence in IBD mucosa augment in vitro utilization of mucin by other bacteria. Am J Gastroenterol **105**:2420–2428.

4. **Vigsnæs LK**, **Brynskov J**, **Steenholdt C**, **Wilcks A**, **Licht TR**. 2012. Gram-negative bacteria account for main differences between faecal microbiota from patients with ulcerative colitis and healthy controls. Benef Microbes **3**:287–297.

5. **Wahlström A**, **Sayin SI**, **Marschall H-U**, **Bäckhed F**. 2016. Intestinal Crosstalk between Bile Acids and Microbiota and Its Impact on Host Metabolism. Cell Metab **24**:41–50.

6. **Kakiyama G**, **Pandak WM**, **Gillevet PM**, **Hylemon PB**, **Heuman DM**, **Daita K**, **Takei H**, **Muto A**, **Nittono H**, **Ridlon JM**, **White MB**, **Noble NA**, **Monteith P**, **Fuchs M**, **Thacker LR**, **Sikaroodi M**, **Bajaj JS**. 2013. Modulation of the fecal bile acid profile by gut microbiota in cirrhosis. J Hepatol **58**:949–955.

7. **Duboc H**, **Rajca S**, **Rainteau D**, **Benarous D**, **Maubert M-A**, **Quervain E**, **Thomas G**, **Barbu V**, **Humbert L**, **Despras G**, **Bridonneau C**, **Dumetz F**, **Grill J-P**, **Masliah J**, **Beaugerie L**, **Cosnes J**, **Chazouillères O**, **Poupon R**, **Wolf C**, **Mallet J-M**, **Langella P**, **Trugnan G**, **Sokol H**, **Seksik P**. 2013. Connecting dysbiosis, bile-acid dysmetabolism and gut inflammation in inflammatory bowel diseases. Gut **62**:531–539.

8. **Calmus Y**, **Weill B**, **Ozier Y**, **Chéreau C**, **Houssin D**, **Poupon R**. 1992. Immunosuppressive properties of chenodeoxycholic and ursodeoxycholic acids in the mouse. Gastroenterology **103**:617–621.

9. **Greve JW**, **Gouma DJ**, **Buurman WA**. 1989. Bile acids inhibit endotoxin-induced release of tumor necrosis factor by monocytes: an in vitro study. Hepatol Baltim Md **10**:454–458.

10. **Yoneno K**, **Hisamatsu T**, **Shimamura K**, **Kamada N**, **Ichikawa R**, **Kitazume MT**, **Mori M**, **Uo M**, **Namikawa Y**, **Matsuoka K**, **Sato T**, **Koganei K**, **Sugita A**, **Kanai T**, **Hibi T**.

2013. TGR5 signalling inhibits the production of pro-inflammatory cytokines by in vitro differentiated inflammatory and intestinal macrophages in Crohn's disease. Immunology **139**:19–29.

11. **Martínez-Moya P**, **Romero-Calvo I**, **Requena P**, **Hernández-Chirlaque C**, **Aranda CJ**, **González R**, **Zarzuelo A**, **Suárez MD**, **Martínez-Augustin O**, **Marín JJG**, **de Medina FS**. 2013. Dose-dependent antiinflammatory effect of ursodeoxycholic acid in experimental colitis. Int Immunopharmacol **15**:372–380.

12. **Invernizzi P**, **Setchell KD**, **Crosignani A**, **Battezzati PM**, **Larghi A**, **O'Connell NC**, **Podda M**. 1999. Differences in the metabolism and disposition of ursodeoxycholic acid and of its taurine-conjugated species in patients with primary biliary cirrhosis. Hepatol Baltim Md **29**:320–327.

13. **Rudolph G**, **Kloeters-Plachky P**, **Sauer P**, **Stiehl A**. 2002. Intestinal absorption and biliary secretion of ursodeoxycholic acid and its taurine conjugate. Eur J Clin Invest **32**:575–580.

14. **Stenman LK**, **Holma R**, **Forsgård R**, **Gylling H**, **Korpela R**. 2013. Higher fecal bile acid hydrophobicity is associated with exacerbation of dextran sodium sulfate colitis in mice. J Nutr **143**:1691–1697.

15. **Cao SS**, **Zimmermann EM**, **Chuang B-M**, **Song B**, **Nwokoye A**, **Wilkinson JE**, **Eaton KA**, **Kaufman RJ**. 2013. The unfolded protein response and chemical chaperones reduce protein misfolding and colitis in mice. Gastroenterology **144**:989–1000.e6.

16. **Laukens D**, **Devisscher L**, **Van den Bossche L**, **Hindryckx P**, **Vandenbroucke RE**, **Vandewynckel Y-P**, **Cuvelier C**, **Brinkman BM**, **Libert C**, **Vandenabeele P**, **De Vos M**.

2014. Tauroursodeoxycholic acid inhibits experimental colitis by preventing early intestinal epithelial cell death. Lab Investig J Tech Methods Pathol **94**:1419–1430.

17. **Kurdi P**, **Kawanishi K**, **Mizutani K**, **Yokota A**. 2006. Mechanism of Growth Inhibition by Free Bile Acids in Lactobacilli and Bifidobacteria. J Bacteriol **188**:1979–1986.

18. **Taranto MP**, **Perez-Martinez G**, **Font de Valdez G**. 2006. Effect of bile acid on the cell membrane functionality of lactic acid bacteria for oral administration. Res Microbiol **157**:720–725.

19. **Sonomoto K**, **Yokota A**. 2011. Lactic Acid Bacteria and Bifidobacteria: Current Progress in Advanced Research. Horizon Scientific Press.

20. **Ridlon JM**, **Alves JM**, **Hylemon PB**, **Bajaj JS**. 2013. Cirrhosis, bile acids and gut microbiota. Gut Microbes **4**:382–387.

21. **Islam KBMS**, **Fukiya S**, **Hagio M**, **Fujii N**, **Ishizuka S**, **Ooka T**, **Ogura Y**, **Hayashi T**, **Yokota A**. 2011. Bile acid is a host factor that regulates the composition of the cecal microbiota in rats. Gastroenterology **141**:1773–1781.

22. **Dürre P**, **Andreesen JR**. 1983. Purine and glycine metabolism by purinolytic clostridia. J Bacteriol **154**:192–199.

23. **Lebertz H**, **Andreesen JR**. 1988. Glycine fermentation by Clostridium histolyticum. Arch Microbiol **150**:11–14.

24. **Laue H**, **Denger K**, **Cook AM**. 1997. Taurine reduction in anaerobic respiration of Bilophila wadsworthia RZATAU. Appl Environ Microbiol **63**:2016–2021.

507 25. **Laue H**, **Smits THM**, **Schumacher UK**, **Claros MC**, **Hartemink R**, **Cook AM**. 2006.
508 Identification of Bilophila wadsworthia by specific PCR which targets the taurine:pyruvate
509 aminotransferase gene. FEMS Microbiol Lett **261**:74–79.

510 26. **Devkota S**, **Wang Y**, **Musch MW**, **Leone V**, **Fehlner-Peach H**, **Nadimpalli A**,
511 **Antonopoulos DA**, **Jabri B**, **Chang EB**. 2012. Dietary-fat-induced taurocholic acid
512 promotes pathobiont expansion and colitis in Il10-/- mice. Nature **487**:104–108.

513 27. **Wlodarska M**, **Kostic AD**, **Xavier RJ**. 2015. An integrative view of microbiome-host
514 interactions in inflammatory bowel diseases. Cell Host Microbe **17**:577–591.

515 28. **Brinkman BM**, **Becker A**, **Ayiseh RB**, **Hildebrand F**, **Raes J**, **Huys G**, **Vandenabeele P**.
516 2013. Gut microbiota affects sensitivity to acute DSS-induced colitis independently of host
517 genotype. Inflamm Bowel Dis **19**:2560–2567.

518 29. **Camarinha-Silva A**, **Jáuregui R**, **Chaves-Moreno D**, **Oxley APA**, **Schaumburg F**,
519 **Becker K**, **Wos-Oxley ML**, **Pieper DH**. 2014. Comparing the anterior nare bacterial
520 community of two discrete human populations using Illumina amplicon sequencing.
521 Environ Microbiol **16**:2939–2952.

522 30. **LANE DJ**. 1991. 16S/23S rRNA sequencing. Nucleic Acid Tech Bact Syst 125–175.

523 31. **Etchebehere C**, **Tiedje J**. 2005. Presence of Two Different Active nirS Nitrite Reductase
524 Genes in a Denitrifying Thauera sp. from a High-Nitrate-Removal-Rate Reactor. Appl
525 Environ Microbiol **71**:5642–5645.

526 32. **Chaves-Moreno D**, **Plumeier I**, **Kahl S**, **Krismer B**, **Peschel A**, **Oxley APA**, **Jauregui R**,
527 **Pieper DH**. 2015. The microbial community structure of the cotton rat nose. Environ
528 Microbiol Rep **7**:929–935.

529 33. **Verstraelen H**, **Vilchez-Vargas R**, **Desimpel F**, **Jauregui R**, **Vankeirsbilck N**, **Weyers S**,
530 **Verhelst R**, **De Sutter P**, **Pieper DH**, **Van De Wiele T**. 2016. Characterisation of the
531 human uterine microbiome in non-pregnant women through deep sequencing of the V1-2
532 region of the 16S rRNA gene. PeerJ **4**:e1602.

533 34. **McMurdie PJ**, **Holmes S**. 2013. phyloseq: An R Package for Reproducible Interactive
534 Analysis and Graphics of Microbiome Census Data. PLOS ONE **8**:e61217.

535 35. **R Core Team**. 2012. R: A language and environment for statistical computing. R
536 Foundation for Statistical Computing, Vienna, Austria.

537 36. **Oksanen J**, **Blanchet FG**, **Friendly M**, **Kindt R**, **Legendre P**, **McGlinn D**, **Minchin PR**,
538 **O'Hara RB**, **Simpson GL**, **Solymos P**, **Stevens MHH**, **Szoecs E**, **Wagner H**. 2016. vegan:
539 Community Ecology Package.

540 37. **Wang Q**, **Garrity GM**, **Tiedje JM**, **Cole JR**. 2007. Naïve Bayesian Classifier for Rapid
541 Assignment of rRNA Sequences into the New Bacterial Taxonomy. Appl Environ
542 Microbiol **73**:5261–5267.

543 38. **Schneeberger M**, **Everard A**, **Gómez-Valadés AG**, **Matamoros S**, **Ramírez S**, **Delzenne**
544 **NM**, **Gomis R**, **Claret M**, **Cani PD**. 2015. Akkermansia muciniphila inversely correlates
545 with the onset of inflammation, altered adipose tissue metabolism and metabolic disorders
546 during obesity in mice. Sci Rep **5**.

39. **Ovreås L**, **Lj F**, **Daae FL**, **Vl T**. 1997. Distribution of bacterioplankton in Meromictic lake Sælenvannet, as determined by denaturing gradient gel electrophoresis of PCR-amplified gene fragments coding for 16S rRNA. Appl Environ Microbiol **63**:3367–73.

40. **Cai X**, **Liu Y**, **Zhou X**, **Navaneethan U**, **Shen B**, **Guo B**. 2012. An LC-ESI-MS method for the quantitative analysis of bile acids composition in fecal materials. Biomed Chromatogr BMC **26**:101–108.

41. **Alex P**, **Zachos NC**, **Nguyen T**, **Gonzales L**, **Chen T-E**, **Conklin LS**, **Centola M**, **Li X**. 2009. Distinct cytokine patterns identified from multiplex profiles of murine DSS and TNBS-induced colitis. Inflamm Bowel Dis **15**:341–352.

42. **Peter MR**, **Jerkic M**, **Sotov V**, **Douda DN**, **Ardelean DS**, **Ghamami N**, **Lakschevitz F**, **Khan MA**, **Robertson SJ**, **Glogauer M**, **Philpott DJ**, **Palaniyar N**, **Letarte M**. 2014. Impaired Resolution of Inflammation in the Endoglin Heterozygous Mouse Model of Chronic Colitis. Mediators Inflamm **2014**.

43. **Rodrigues CM**, **Kren BT**, **Steer CJ**, **Setchell KD**. 1995. Tauroursodeoxycholate increases rat liver ursodeoxycholate levels and limits lithocholate formation better than ursodeoxycholate. Gastroenterology **109**:564–572.

44. **Alnouti Y**, **Csanaky IL**, **Klaassen CD**. 2008. Quantitative-Profiling of Bile Acids and their Conjugates in Mouse Liver, Bile, Plasma, and Urine Using LC-MS/MS. J Chromatogr B Analyt Technol Biomed Life Sci **873**:209–217.

566 45. **Nagalingam NA**, **Kao JY**, **Young VB**. 2011. Microbial ecology of the murine gut
567 associated with the development of dextran sodium sulfate-induced colitis. Inflamm Bowel
568 Dis **17**:917–926.

569 46. **Schwab C**, **Berry D**, **Rauch I**, **Rennisch I**, **Ramesmayer J**, **Hainzl E**, **Heider S**, **Decker**
570 **T**, **Kenner L**, **Müller M**, **Strobl B**, **Wagner M**, **Schleper C**, **Loy A**, **Urich T**. 2014.
571 Longitudinal study of murine microbiota activity and interactions with the host during acute
572 inflammation and recovery. ISME J **8**:1101–1114.

573 47. **Manichanh C**, **Rigottier-Gois L**, **Bonnaud E**, **Gloux K**, **Pelletier E**, **Frangeul L**, **Nalin**
574 **R**, **Jarrin C**, **Chardon P**, **Marteau P**, **Roca J**, **Dore J**. 2006. Reduced diversity of faecal
575 microbiota in Crohn's disease revealed by a metagenomic approach. Gut **55**:205–211.

576 48. **Wills ES**, **Jonkers DMAE**, **Savelkoul PH**, **Masclee AA**, **Pierik MJ**, **Penders J**. 2014.
577 Fecal Microbial Composition of Ulcerative Colitis and Crohn's Disease Patients in
578 Remission and Subsequent Exacerbation. PLOS ONE **9**:e90981.

579 49. **Gerritsen J**, **Smidt H**, **Rijkers GT**, **de Vos WM**. 2011. Intestinal microbiota in human
580 health and disease: the impact of probiotics. Genes Nutr **6**:209–240.

581 50. **Le Chatelier E**, **Nielsen T**, **Qin J**, **Prifti E**, **Hildebrand F**, **Falony G**, **Almeida M**,
582 **Arumugam M**, **Batto J-M**, **Kennedy S**, **Leonard P**, **Li J**, **Burgdorf K**, **Grarup N**,
583 **Jørgensen T**, **Brandslund I**, **Nielsen HB**, **Juncker AS**, **Bertalan M**, **Levenez F**, **Pons N**,
584 **Rasmussen S**, **Sunagawa S**, **Tap J**, **Tims S**, **Zoetendal EG**, **Brunak S**, **Clément K**, **Doré**
585 **J**, **Kleerebezem M**, **Kristiansen K**, **Renault P**, **Sicheritz-Ponten T**, **de Vos WM**, **Zucker**
586 **J-D**, **Raes J**, **Hansen T**, **MetaHIT consortium**, **Bork P**, **Wang J**, **Ehrlich SD**, **Pedersen**

O. 2013. Richness of human gut microbiome correlates with metabolic markers. Nature **500**:541–546.

51. **Vandeputte D**, **Falony G**, **Vieira-Silva S**, **Tito RY**, **Joossens M**, **Raes J**. 2016. Stool consistency is strongly associated with gut microbiota richness and composition, enterotypes and bacterial growth rates. Gut **65**:57–62.

52. **Ley RE**, **Turnbaugh PJ**, **Klein S**, **Gordon JI**. 2006. Microbial ecology: Human gut microbes associated with obesity. Nature **444**:1022–1023.

53. **Hong SN**, **Rhee P-L**. 2014. Unraveling the ties between irritable bowel syndrome and intestinal microbiota. World J Gastroenterol WJG **20**:2470–2481.

54. **Wen L**, **Ley RE**, **Volchkov PV**, **Stranges PB**, **Avanesyan L**, **Stonebraker AC**, **Hu C**, **Wong FS**, **Szot GL**, **Bluestone JA**, **Gordon JI**, **Chervonsky AV**. 2008. Innate immunity and intestinal microbiota in the development of Type 1 diabetes. Nature **455**:1109–1113.

55. **Brinkman BM**, **Hildebrand F**, **Kubica M**, **Goosens D**, **Del Favero J**, **Declercq W**, **Raes J**, **Vandenabeele P**. 2011. Caspase deficiency alters the murine gut microbiome. Cell Death Dis **2**:e220.

56. **Ritchie LE**, **Sturino JM**, **Carroll RJ**, **Rooney LW**, **Azcarate-Peril MA**, **Turner ND**. 2015. Polyphenol-rich sorghum brans alter colon microbiota and impact species diversity and species richness after multiple bouts of dextran sodium sulfate-induced colitis. FEMS Microbiol Ecol **91**.

57. **Kabeerdoss J**, **Jayakanthan P**, **Pugazhendhi S**, **Ramakrishna BS**. 2015. Alterations of mucosal microbiota in the colon of patients with inflammatory bowel disease revealed by

real time polymerase chain reaction amplification of 16S ribosomal ribonucleic acid. Indian J Med Res **142**:23–32.

58. **Verdam FJ**, **Fuentes S**, **de Jonge C**, **Zoetendal EG**, **Erbil R**, **Greve JW**, **Buurman WA**, **de Vos WM**, **Rensen SS**. 2013. Human intestinal microbiota composition is associated with local and systemic inflammation in obesity. Obes Silver Spring Md **21**:E607-615.

59. **Lau E**, **Marques C**, **Pestana D**, **Santoalha M**, **Carvalho D**, **Freitas P**, **Calhau C**. 2016. The role of I-FABP as a biomarker of intestinal barrier dysfunction driven by gut microbiota changes in obesity. Nutr Metab **13**.

60. **De Fazio L**, **Cavazza E**, **Spisni E**, **Strillacci A**, **Centanni M**, **Candela M**, **Praticò C**, **Campieri M**, **Ricci C**, **Valerii MC**. 2014. Longitudinal analysis of inflammation and microbiota dynamics in a model of mild chronic dextran sulfate sodium-induced colitis in mice. World J Gastroenterol **20**:2051–2061.

61. **Wang W**, **Chen L**, **Zhou R**, **Wang X**, **Song L**, **Huang S**, **Wang G**, **Xia B**. 2014. Increased proportions of Bifidobacterium and the Lactobacillus group and loss of butyrate-producing bacteria in inflammatory bowel disease. J Clin Microbiol **52**:398–406.

62. **Machiels K**, **Joossens M**, **Sabino J**, **De Preter V**, **Arijs I**, **Eeckhaut V**, **Ballet V**, **Claes K**, **Van Immerseel F**, **Verbeke K**, **Ferrante M**, **Verhaegen J**, **Rutgeerts P**, **Vermeire S**. 2014. A decrease of the butyrate-producing species Roseburia hominis and Faecalibacterium prausnitzii defines dysbiosis in patients with ulcerative colitis. Gut **63**:1275–1283.

628 63. **Hirano S**, **Masuda N**. 1982. Enhancement of the 7 alpha-dehydroxylase activity of a gram-
629 positive intestinal anaerobe by Bacteroides and its significance in the 7-dehydroxylation of
630 ursodeoxycholic acid. J Lipid Res **23**:1152–1158.

631 64. **Lepercq P**, **Gérard P**, **Béguet F**, **Grill J-P**, **Relano P**, **Cayuela C**, **Juste C**. 2004. Isolates
632 from Normal Human Intestinal Flora but not Lactic Acid Bacteria Exhibit 7a- and 7b-
633 Hydroxysteroid Dehydrogenase Activities. Microb Ecol Health Dis **16**:195–201.

634 65. **Atarashi K**, **Tanoue T**, **Shima T**, **Imaoka A**, **Kuwahara T**, **Momose Y**, **Cheng G**,
635 **Yamasaki S**, **Saito T**, **Ohba Y**, **Taniguchi T**, **Takeda K**, **Hori S**, **Ivanov II**, **Umesaki Y**,
636 **Itoh K**, **Honda K**. 2011. Induction of colonic regulatory T cells by indigenous Clostridium
637 species. Science **331**:337–341.

638 66. **Barcenilla A**, **Pryde SE**, **Martin JC**, **Duncan SH**, **Stewart CS**, **Henderson C**, **Flint HJ**.
639 2000. Phylogenetic Relationships of Butyrate-Producing Bacteria from the Human Gut.
640 Appl Environ Microbiol **66**:1654–1661.

641 67. **Di Sabatino A**, **Morera R**, **Ciccocioppo R**, **Cazzola P**, **Gotti S**, **Tinozzi FP**, **Tinozzi S**,
642 **Corazza GR**. 2005. Oral butyrate for mildly to moderately active Crohn's disease. Aliment
643 Pharmacol Ther **22**:789–794.

644 68. **Kumari R**, **Ahuja V**, **Paul J**. 2013. Fluctuations in butyrate-producing bacteria in
645 ulcerative colitis patients of North India. World J Gastroenterol **19**:3404–3414.

646 69. **Klinkspoor JH**, **Tytgat GN**, **Lee SP**, **Groen AK**. 1996. Mechanism of bile salt-induced
647 mucin secretion by cultured dog gallbladder epithelial cells. Biochem J **316**:873–877.

70. **Shekels LL**, **Lyftogt CT**, **Ho SB**. 1996. Bile acid-induced alterations of mucin production in differentiated human colon cancer cell lines. Int J Biochem Cell Biol **28**:193–201.

71. **Klinkspoor JH**, **Mok KS**, **Van Klinken BJ**, **Tytgat GN**, **Lee SP**, **Groen AK**. 1999. Mucin secretion by the human colon cell line LS174T is regulated by bile salts. Glycobiology **9**:13–19.

72. **Derrien M**, **van Passel MW**, **van de Bovenkamp JH**, **Schipper RG**, **de Vos WM**, **Dekker J**. 2010. Mucin-bacterial interactions in the human oral cavity and digestive tract. Gut Microbes **1**:254–268.

73. **Derrien M**, **Van Baarlen P**, **Hooiveld G**, **Norin E**, **Müller M**, **de Vos WM**. 2011. Modulation of Mucosal Immune Response, Tolerance, and Proliferation in Mice Colonized by the Mucin-Degrader Akkermansia muciniphila. Front Microbiol **2**:166.

74. **Everard A**, **Belzer C**, **Geurts L**, **Ouwerkerk JP**, **Druart C**, **Bindels LB**, **Guiot Y**, **Derrien M**, **Muccioli GG**, **Delzenne NM**, **Vos WM de**, **Cani PD**. 2013. Cross-talk between Akkermansia muciniphila and intestinal epithelium controls diet-induced obesity. Proc Natl Acad Sci **110**:9066–9071.

75. **Ridgway N**, **McLeod R**. 2015. Biochemistry of Lipids, Lipoproteins and Membranes. Elsevier.

76. **Nguyen TLA**, **Vieira-Silva S**, **Liston A**, **Raes J**. 2015. How informative is the mouse for human gut microbiota research? Dis Model Mech **8**:1–16.

667 77. **Roma MG**, **Toledo FD**, **Boaglio AC**, **Basiglio CL**, **Crocenzi FA**, **Sánchez Pozzi EJ**.
668 2011. Ursodeoxycholic acid in cholestasis: linking action mechanisms to therapeutic
669 applications. Clin Sci Lond Engl 1979 **121**:523–544.

670 78. **Pardi DS**, **Loftus Jr EV**, **Kremers WK**, **Keach J**, **Lindor KD**. 2003. Ursodeoxycholic
671 acid as a chemopreventive agent in patients with ulcerative colitis and primary sclerosing
672 cholangitis. Gastroenterology **124**:889–893.

673 79. **Kohno H**, **Suzuki R**, **Yasui Y**, **Miyamoto S**, **Wakabayashi K**, **Tanaka T**. 2007.
674 Ursodeoxycholic Acid versus Sulfasalazine in Colitis-Related Colon Carcinogenesis in
675 Mice. Am Assoc Cancer Res **13**:2519–2525.

676 80. **Huang W-K**, **Hsu H-C**, **Liu J-R**, **Yang T-S**, **Chen J-S**, **Chang JW-C**, **Lin Y-C**, **Yu K-H**,
677 **Kuo C-F**, **See L-C**. 2016. The Association of Ursodeoxycholic Acid Use With Colorectal
678 Cancer Risk. Medicine (Baltimore) **95**.

679

680 **FIGURE LEGENDS**

681 **Figure 1. Oral administration of UDCA, TUDCA and GUDCA improves clinical**
682 **parameters and inflammatory markers in acute DSS-induced colitis.** C57BL/6J mice
683 received 4% DSS in the drinking water for 7 days, followed by normal water for 3 days. Control
684 mice received water alone. From the start of DSS administration, mice were treated with UDCA,
685 TUDCA or GUDCA (500 mg/kg/d) by oral gavage. **(A)** Body weight changes during acute DSS-
686 induced colitis. Body weights are represented as a percentage of their initial body weight at day
687 0. Results of a Mann-Whitney U test on day 10 are shown. **(B)** Clinical disease activity score.
688 Results of a Mann-Whitney U test on day 9 are shown. **(C)** Colon lengths were assessed upon

689 euthanasia on day 10. **(D,E)** Cytokine levels of CXCL1, G-CSF and IL-6 in colonic tissue (D)
690 and serum (E) collected on day 10. Data are represented as the mean ± SEM (n = 8 in each
691 group). *P<0.05, **P<0.01. C = Control; P = Placebo; T = TUDCA; U = UDCA; G = GUDCA.

692 **Figure 2. Oral administration of UDCA, TUDCA and GUDCA during DSS-induced colitis**
693 **prevents colitis-associated dysbiosis at the phylum level.** Fecal samples were collected on day
694 9 of colitis and microbiota profiles were characterized by 16S rRNA Illumina MiSeq sequencing.
695 **(A-C)** Estimation of (A) species richness (i.e., total number of operational taxonomic units), (B)
696 species diversity (i.e., Shannon index) and (C) bacterial load in the fecal microbiota. Bacterial
697 load was calculated as $2^{deltaCt}$ / [total DNA concentration]. **(D)** Ratio of the percentage of 16S
698 rRNA gene sequences belonging to *Firmicutes* and *Bacteroidetes*. **(E)** Composition of the fecal
699 microbial community at the phylum level. Data are represented as the mean ± SEM (n ≥ 6 in each
700 group). *P<0.05, **P<0.01. C = Control; P = Placebo; T = TUDCA; U = UDCA; G = GUDCA.

701 **Figure 3. Oral administration of UDCA, TUDCA and GUDCA during DSS-induced colitis**
702 **alters the fecal microbiota at lower taxonomic levels.** Fecal samples were collected on day 9 of
703 colitis and microbiota profiles were characterized by 16S rRNA Illumina MiSeq sequencing. **(A)**
704 Composition of the fecal microbial community at the class level. **(B-F)** Percentage of 16S rRNA
705 gene sequences belonging to (B) *Bacteroidaceae*, (C) *Porphyromonadaceae,* (D) *Prevotellaceae*,
706 (E) *Clostridium* cluster XIVa and (F) *Akkermansia.* (**G**) qRT-PCR results for *A. muciniphila*.
707 Copy numbers were normalized to the 16S rRNA gene copy number in each sample. Data are
708 represented as the mean ± SEM (n ≥ 6 in each group). *P<0.05, **P<0.01. C = Control; P =
709 Placebo; T = TUDCA; U = UDCA; G = GUDCA.

710 **Figure 4. Orally administered UDCA, TUDCA and GUDCA undergo extensive**
711 **biotransformation.** Fecal samples were collected at day 4 of colitis and bile acids were
712 quantified using UHPLC-HRMS. **(A)** UDCA, **(B)** TUDCA, **(C)** LCA and **(D)** GUDCA. Data are

represented as the mean ± SEM (n ≥ 7 in each group). *P<0.05, **P<0.01. C = Control; P = Placebo; T = TUDCA; U = UDCA; G = GUDCA.

Figure 1

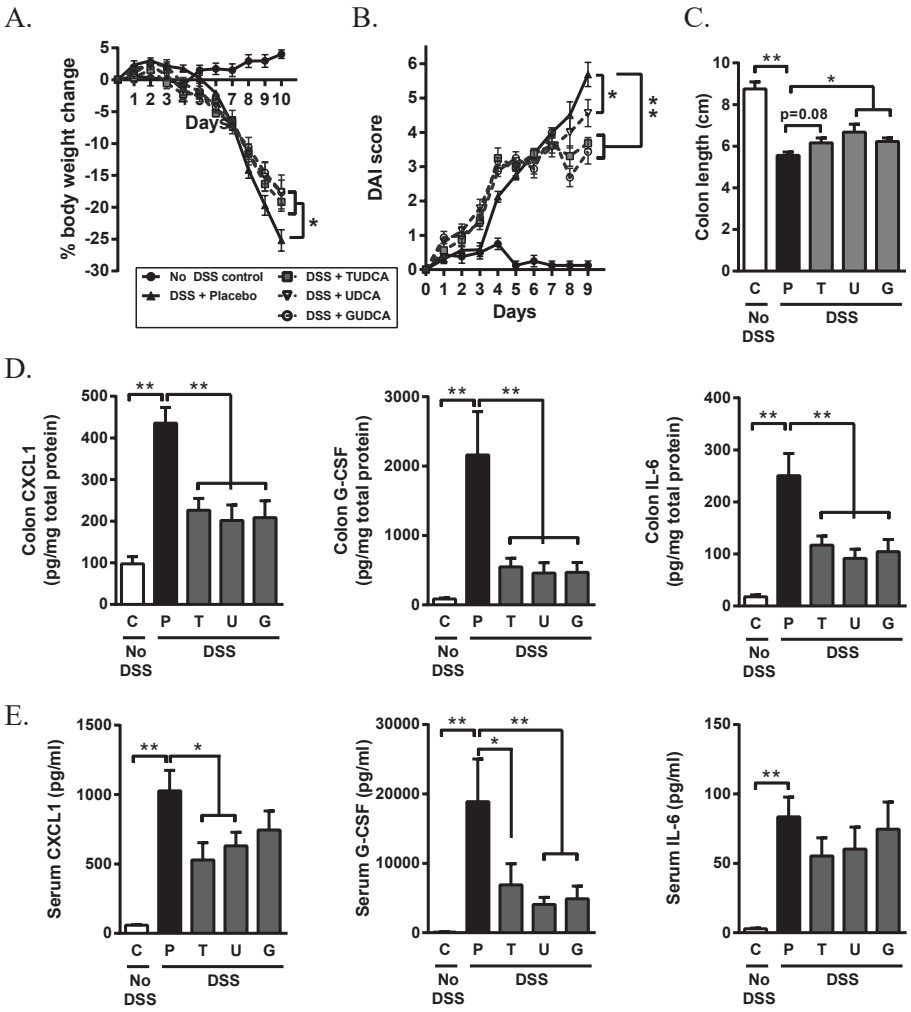

Figure 2

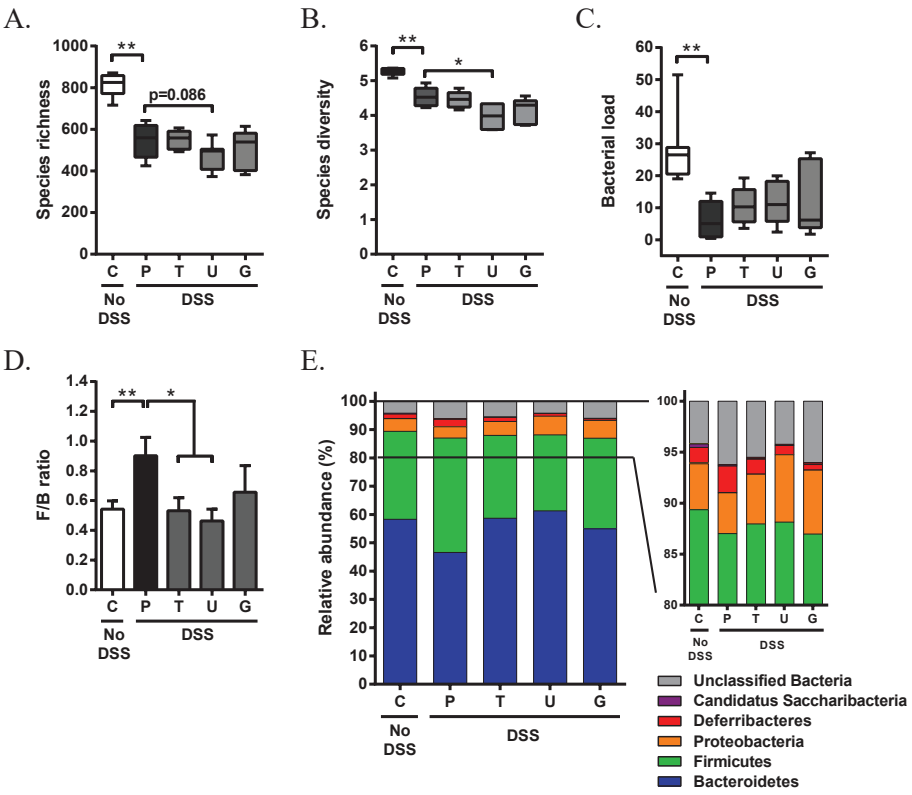

Figure 3

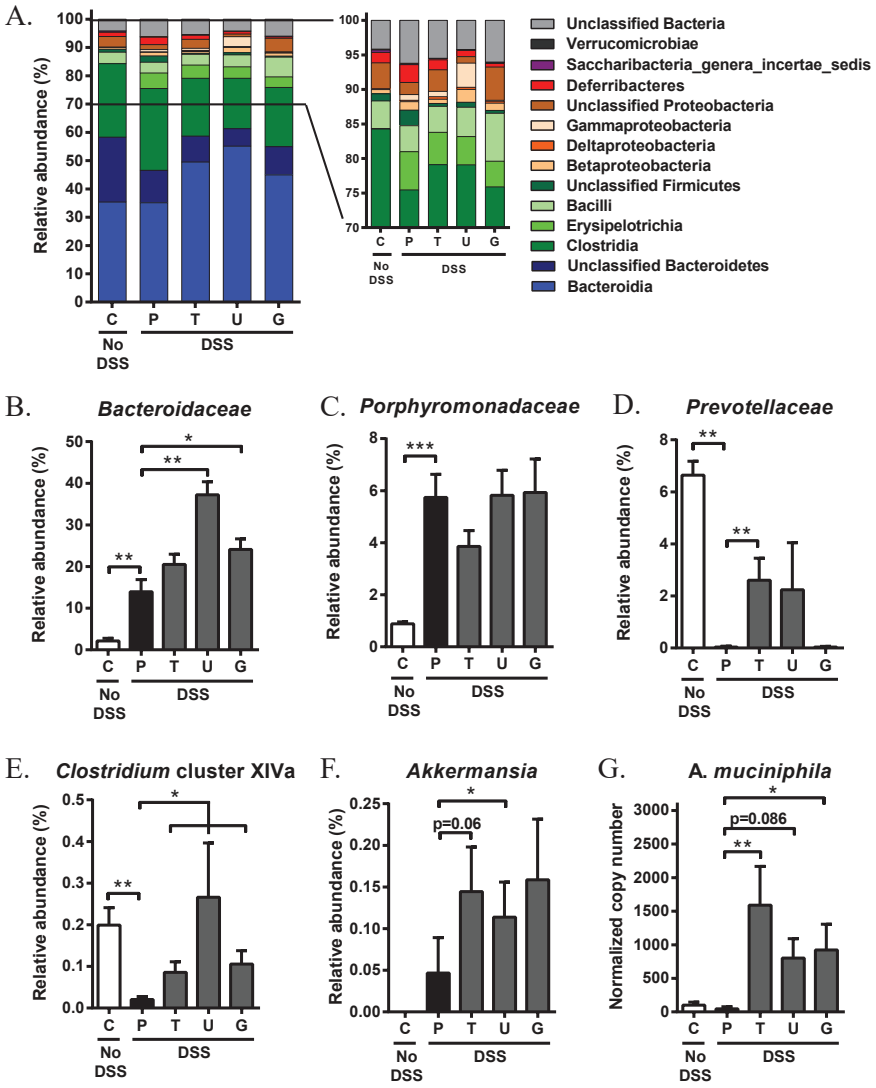

Figure 4